

# Smad4 and Trim33/Tif1 $\gamma$ Redundantly Regulate Neural Stem Cells in the Developing Cortex

Sven Falk<sup>1,3</sup>, Esm e Joosten<sup>1</sup>, Vesa Kaartinen<sup>2</sup> and Lukas Sommer<sup>1</sup>

<sup>1</sup>Division of Cell and Developmental Biology, Institute of Anatomy, University of Zurich, Zurich, Switzerland, <sup>2</sup>Department of Biologic and Materials Sciences, University of Michigan, Ann Arbor, MI 48109, USA and <sup>3</sup>Current address: Helmholtz Center Munich, German Research Center for Environmental Health, Institute for Stem Cell Research, D-85764 Neuherberg, Germany

Address correspondence to Lukas Sommer. Email: lukas.sommer@anatom.uzh.ch

**During central nervous system (CNS) development, proliferation and differentiation of neural stem cells (NSCs) have to be regulated in a spatio-temporal fashion. Here, we report different branches of the transforming growth factor  $\beta$  (TGF $\beta$ ) signaling pathway to be required for the brain area-specific control of NSCs. In the midbrain, canonical TGF $\beta$  signaling via Smad4 regulates the balance between proliferation and differentiation of NSCs. Accordingly, Smad4 deletion resulted in horizontal expansion of NSCs due to increased proliferation, decreased differentiation, and decreased cell cycle exit. In the developing cortex, however, ablation of Smad4 alone did not have any effect on proliferation and differentiation of NSCs. In contrast, concomitant mutation of both Smad4 and Trim33 led to an increase in proliferative cells in the ventricular zone due to decreased cell cycle exit, revealing a functional redundancy of Smad4 and Trim33. Furthermore, in Smad4-Trim33 double mutant embryos, cortical NSCs generated an excess of deep layer neurons concurrent with a delayed and reduced production of upper layer neurons and, in addition, failed to undergo the neurogenic to gliogenic switch at the right developmental stage. Thus, our data disclose that in different regions of the developing CNS different aspects of the TGF $\beta$  signaling pathway are required to ensure proper development.**

**Keywords:** brain development, cortex, neural stem cells, Smad4, Trim33

## Introduction

In the developing central nervous system (CNS), self-renewing and multipotent neural stem cells (NSCs) are the primary source for all neurons, astrocytes, and oligodendrocytes present at mature stages. Early in development, before the onset of neurogenesis, the division mode of NSCs is a symmetric proliferative one, generating 2 NSCs from 1 mother stem cell and thereby expanding the neuroepithelium horizontally (Gotz and Huttner 2005; Kriegstein and Alvarez-Buylla 2009). Later, the division mode switches to asymmetric cell divisions, whereby a NSC gives rise to another NSC and a differentiating cell. To ensure proper development of the CNS not only the number of NSCs, but also the number and kind of their progeny has to be tightly regulated (Rakic 1995, 2009). In the developing cortex of mice, neurogenesis starts around embryonic day 11 (E11) and is followed by the generation of glial cells after E18 (Miller and Gauthier 2007). The production of neurons follows a stereotypic sequence by which neurons arise in a layer-specific order from deep layer neurons (layer 5 and 6) to upper layer neurons (layer 2 and 3) (Angevine and Sidman 1961; Rakic 1974). Therefore, the time of birth of a neuron determines its particular laminar fate.

Several factors have been implicated in this temporal regulation of NSCs (Okano and Temple 2009), such as Sip1, a protein thought to regulate the transforming growth factor  $\beta$  (TGF $\beta$ ) pathway by interacting with receptor-activated Smads

(R-Smads) (Seuntjens et al. 2009). The canonical TGF $\beta$  pathway is activated by cytokines of the TGF $\beta$  superfamily. Upon ligand binding, the receptor type I phosphorylates the receptor type II, which in turn propagates the signal by phosphorylation of R-Smads. Activated R-Smads form a complex with the common-Smad, Smad4, and translocate to the nucleus where they regulate target gene transcription (Massague 2008). While different branches of the Smad pathway utilize different R-Smads, they all share Smad4 as a central component of the canonical pathway. Trim33/Tif1 $\gamma$  is a molecule implicated in regulation of the TGF $\beta$  signaling pathway activity by modulating Smad4 action. It has been reported that Trim33 competes with Smad4 for interaction with receptor-activated Smad2/3 (He et al. 2006) and that the 2 complexes (Smad4-Smad2/3 and Trim33-Smad2/3) cooperate in regulating target gene expression (Xi et al. 2011). However, depending on the context, Trim33 can also act as an inhibitor of Smad4 function (Dupont et al. 2005, 2009; Morsut et al. 2010).

Besides the temporal regulation of neural development, the progenitor cells in the developing CNS have also to be patterned area specifically in order to produce specialized regions. A classical model for nervous system development suggests that a proto-map of CNS areas is setup in the early developing neuroepithelium (Rakic 1988). Several different signaling pathways have been shown to extrinsically instruct regional growth in the CNS, including WNTs and FGFs (Grove et al. 1998; Fukuchi-Shimogori and Grove 2001; Shimogori et al. 2004; Cholfin and Rubenstein 2007; O'Leary et al. 2007). Importantly, signaling by TGF $\beta$  superfamily members is one of the key signaling pathways conferring positional information to this proto-map in the developing cortex at early developmental stages (Shimamura and Rubenstein 1997; Barth et al. 1999; Shimogori et al. 2004; Caronia et al. 2010). At later developmental stages, TGF $\beta$ 1 is expressed in the choroid plexus, suggesting a long-range action of the ligand on distant receiving cells through the cerebrospinal fluid (Falk et al. 2008). Interestingly, signaling via the TGF $\beta$  receptor type II regulates proliferation, differentiation, and cell cycle exit of NSCs specifically in the dorsal midbrain, but not in the ventral midbrain or the dorsal forebrain (Falk et al. 2008), revealing an area-specific readout.

Here, we show that in distinct regions of the CNS, different features of the TGF $\beta$  signaling pathway are required to ensure proper development. Smad4, the central component of the canonical TGF $\beta$  signaling pathway, is required to control proliferation, differentiation, and cell cycle exit in both the dorsal and the ventral midbrain. By contrast, in the dorsal forebrain, Smad4 ablation had no effect on the balance between proliferation and differentiation of NSCs. However, when combined with conditional inactivation of Trim33, Smad4 ablation in the developing cortex led to an increase in proliferative cells in the

ventricular zone and to decreased cell cycle exit, very much resembling the phenotype of the *Smad4*-ablated midbrain. Moreover, *Smad4* and *Trim33* together are required for the proper temporal progression of NSCs in the forebrain.

## Materials and Methods

### Generation of Mutant Mice and In Vivo Fate Mapping

To conditionally delete the gene of interest in a given tissue the *Cre/loxP* system was used. Animals homozygous for the floxed *Smad4* allele (Yang et al. 2002) and/or the floxed *Trim33* allele (Kim and Kaartinen 2008) were mated with mice heterozygous for the respective floxed allele(s) and carrying the *Cre*-recombinase. For recombination in the dorsal forebrain, the *Emx1Cre* knock-in allele (Gorski et al. 2002) (obtained from Jackson Laboratory) was used while the *Wnt1Cre* transgene (Danielian et al. 1998) drove the recombination in the midbrain. For in vivo fate mapping of recombined cells and to monitor *Cre*-mediated recombination in general, the *R26R* allele (Soriano 1999) was employed. For timed matings, male and female mice were put together in a cage overnight. If a female was pregnant midnight of this night was considered E0. The phenotypes described were 100% penetrant in mutant animals. Littermates carrying one wild-type allele or lacking *Cre* displayed no overt phenotype and were used as controls. *Wnt1Cre-Smad4* conditional knockouts died shortly after E12.5, most probably due to defects in heart tissue derived from neural crest cells that are also recombined by *Wnt1Cre* (Ko et al. 2007; Buchmann-Moller et al. 2009). *Emx1Cre-Smad4-Trim33* mutant animals were born at the expected Mendelian ratio, but died shortly after birth resulting in an under-representation of double mutants at postnatal stages. All animal experiments were approved by the veterinary office of the Canton of Zurich, Switzerland. Genotyping was done by PCR on genomic DNA. DNA for was prepared as described (Truett et al. 2000), and the reactions were carried out as described here (Yang et al. 2002; Falk et al. 2008; Kim and Kaartinen 2008).

### Immunohistochemistry

Tissue was dissected in phosphate buffered saline (PBS) and fixed in 4% para-formaldehyde (PFA) in diethylpyrocarbonate-PBS (DEPC-PBS). For embedding in optimal cutting temperature compound and subsequent cryo sectioning, embryos were put in 30% sucrose (in DEPC-PBS) overnight. For embedding in paraffin, the fixed tissue was serially dehydrated (30% ethanol [EtOH], 50% EtOH, 70% EtOH) and subsequently processed in the STP-120 Spin Tissue Processor (Microm International) and then embedded in paraffin. Immunohistochemistry was performed on 12  $\mu$ m cryo-sections or 5  $\mu$ m paraffin-sections according to supplementary Table S1. Where necessary, antigen retrieval was performed in either 10 mM citrate buffer pH6 (10 mM citric acid, pH6) or 10 mM Tris-EDTA buffer pH9 (10 mM Tris base, 1 mM EDTA Solution, pH 9.0) using the high-pressure cooker device Rapid Microwave Histoprocessor, HistosPRO (SW 2.0.0). Blocking and antibody incubation was done in blocking buffer (10% heat-inactivated goat serum, 0.1% Tween-20, PBS). Standard fluorescence-conjugated secondary antibodies from Jackson ImmunoResearch and Molecular Probes/Invitrogen were used. Stainings for *Smad4* were done with the TSA Plus Cyanine 3 System from Perkin Elmer according to the manufacturer's instructions. TUNEL staining was performed following the producer's guidelines (Roche Diagnostics). All sections were counterstained with 4',6-diamidino-2-phenylindole, dihydrochloride.

### BrdU Labeling

5-Bromo-2'-deoxyuridine (BrdU) labeling was performed by i.p. injection of 10  $\mu$ l/g body weight of the pregnant mother of 10 mM BrdU solution. For the analysis of the cell cycle exit, mice were injected 20 h before they were sacrificed. At least 4 sections from each embryo were analyzed and averaged. As the antibodies used bind BrdU only in single stranded DNA, the sections were incubated in 2 N HCl for 30 min to denature the DNA, followed by neutralization with 0.1 M Na-tetraborate (pH 8.5) for 30 min and washing in PBS.

### RNA In Situ Hybridization

Cryo-sections (12  $\mu$ m) were warmed to room temperature and post-fixed in RNase-free 4% PFA for 10 min. For RNA in situ hybridization on paraffin sections, the slides were deparaffinized and then post-fixed like the cryo-sections. All further steps are identical whether paraffin or cryo-sections were used. To whiten the tissue, the sections were incubated for 15 min in 6% H<sub>2</sub>O<sub>2</sub>. Optionally, sections from embryos older than E14 were treated 50  $\mu$ g/ $\mu$ l Proteinase K (in 50 mM Tris-HCl, 5 mM EDTA, pH 7.5) for 10 min. Acetylation was performed in 0.1 M triethanolamine pH8 with 0.25% acetic anhydride for 10 min. The sections were incubated at least for 4 h at 65 °C in prewarmed hybridization solution (50% formamide, 5 $\times$  SSC, 1 mg/ml yeast tRNA, 100  $\mu$ g/ml heparin, 1 $\times$  Denhardt's Solution, 0.1% Tween-20, 0.1% CHAPS, 5 mM EDTA). Incubation with DIG-labeled RNA antisense probes in hybridization solution (prewarmed) was done at 65 °C for at least 16 h. This was followed by washing once in 1.5 $\times$  SSC at 65°C for 15 min, twice in 2 $\times$  SSC at 37 °C for 30 min, then treatment with 0.5  $\mu$ g/ml RNase A in 2 $\times$  SSC for 30 min at 37 °C, followed by further washing steps twice in 2 $\times$  SSC 30 min at room temperature, twice in 0.2 $\times$  SSC 30 min at 65 °C, and twice in TBST (500 mM NaCl, 20 mM Tris-HCl, 1% Tween-20, pH7.5) at room temperature for 30 min. Blocking was done for 4–6 h at room temperature in 20% lamb serum in TBST and was followed by incubation with anti DIG-AP antibody (see supplementary Table S1) in TBST with 20% lamb serum overnight at 4 °C. After washing twice in TBST for 30 min and twice in alkaline phosphatase (AP) buffer (100 mM Tris-HCl, 50 mM MgCl<sub>2</sub>, 100 mM NaCl, 0.1% Tween-20, 5 mM Levamisole, pH9.5) for 10 min, the color reaction was performed in AP buffer containing 0.35% BCIP (Roche) and 0.1% NBT (Roche) in the dark at 37 °C until it reached a satisfactory intensity. The reaction was stopped by placing the slides in PBS, followed by fixation in MEMFA (0.1 M MOPS pH7.5, 2 mM EGTA, 1 mM MgSO<sub>4</sub>, 3.7% formaldehyde). Riboprobes used were in vitro transcribed from plasmids. The following probes were used: *wnt1* (gift of R. Nusse), *otx2* (gift of J. Rossant).

### X-Gal Staining

Unfixed embryos and brains were incubated in staining solution (5 mM K<sub>3</sub>Fe(CN)<sub>6</sub>, 5 mM K<sub>4</sub>Fe(CN)<sub>6</sub>, 2 mM MgCl<sub>2</sub>, 0.02% NP-40, in PBS, 1 mg/ml X-Gal). Optionally, the tissue can be slightly fixed in a weak fixative (2% formaldehyde, 0.2% glutaraldehyde, 0.02% NP-40 in PBS) before commencing the staining procedure.

### Microscopy and Image Analysis

Epifluorescent and bright field pictures were acquired with the inverse fluorescence microscope Leica DMI6000 B (Leica, Germany). Confocal pictures were taken with the confocal laser-scanning microscopes CLSM SP2 (upright, Leica, Germany) and CLSM SP5 (inverse, Leica, Germany).

ImageJ (<http://rsbweb.nih.gov/ij/>) and Adobe Photoshop CS5 were used for standard image processing tasks. ImageJ was used to quantify cell numbers in a given tissue, taking advantage of the *IITCN* and *cell counter* plug-in available in ImageJ. Distances were measured with the "measure" plug-in native to ImageJ. In the midbrain neuroepithelial stretches of variable length have been analyzed on sagittal sections and normalized to 100  $\mu$ m of apical extension. In the cortex, on coronal sections, medial structures including the hippocampal primordium were excluded from quantifications while the lateral structures were taken into account. Numbers were normalized to 100  $\mu$ m of apical surface, defining a radial unit. Imaris (Bitplane, Switzerland) was used for the processing of stacks acquired with a confocal laser-scanning microscope.

### Statistical Analysis

Each experiment was performed with at least 3 independent samples. Results are shown as mean  $\pm$  standard error of the mean. Statistical significance was tested with the unpaired 2-tailed Student's *t*-test. Calculations of the standard deviation as well as the *P*-value were done using Microsoft Excel.

## Results

In the dorsal midbrain, TGF $\beta$  signaling is a key component in a signaling network controlling NSC numbers by controlling the self-renewal of NSCs (Falk et al. 2008). However, these regulatory mechanisms are operating in a brain area-specific manner. Neither in the ventral midbrain nor in the dorsal forebrain an effect on the stem cell pool could be observed upon interference with the pathway at the level of the receptor Tgfbr2 (Falk et al. 2008). This could be due to redundancy with other TGF $\beta$  superfamily members, such as Activin $\beta$ B, which is expressed in the ventral midbrain and the dorsal forebrain (Feijen et al. 1994). While Activins and TGF $\beta$ s use distinct receptor dimers for signaling, they share the same canonical intracellular signaling mediators Smad2, Smad3, and Smad4 (Massague 2008). To circumvent potential redundancy between different TGF $\beta$  superfamily members, we have chosen to conditionally ablate *Smad4* in the dorsal and ventral midbrain as well as in the dorsal forebrain.

### ***Smad4* Mutation Leads to Massive Enlargement of the Dorsal and Ventral Midbrain**

To inactivate the Smad4 protein, we took advantage of the Cre/loxP system using a conditional allele of *Smad4*, in which exon 8 is flanked by *LoxP* sites (Yang et al. 2002). Exon8 encodes the N-terminal part of the MH2 domain responsible for interaction of Smad4 with phosphorylated R-Smads and other transcriptional co-regulators (Yang et al. 2002). Recombination by Cre-recombinase leads to excision of exon 8 and therefore to a truncated *Smad4* gene, which ultimately leads to a null-mutant (Yang et al. 2002; Buchmann-Moller et al. 2009). Smad4 is expressed ubiquitously in the CNS at E11.5 (Fig. 1A), including the entire midbrain and forebrain. *Wnt1Cre*-mediated deletion of *Smad4* in the midbrain (Danielian et al. 1998; Falk et al. 2008) abolished Smad4 protein expression at E11.5 (Fig. 1B), thus blocking canonical TGF $\beta$  signaling. While at this stage, the overall morphology of the mutant midbrain appeared to be normal, the neuroepithelium of the midbrain at E12.5 showed a dramatic lateral expansion, which was so extensive that the normally smooth midbrain formed undulating folds (Fig. 1C,D).

The morphological changes observed in *Smad4*-cko midbrain and hindbrain raised the question of whether this is partially due to mispatterning in that region. The mid/hindbrain boundary is a powerful signaling center, important early in development to control the identity of adjacent brain regions. However, the transcription factors *Otx2* and *Pax2*, important patterning molecules expressed in specific domains at the mid/hindbrain boundary (Rowitch and McMahon 1995; Broccoli et al. 1999), did not show any change in their expression patterns (Supplementary Fig. 1A,B). Expansion of tissue might also involve decreased packaging of cells. However, cell density was unaltered in the ventral midbrain (co:  $0.0157 \pm 0.0013$  nuclei/ $\mu\text{m}^2$ ; *Wnt1Cre-Smad4*:  $0.0164 \pm 0.0005$  nuclei/ $\mu\text{m}^2$ ;  $n = 4$ ;  $P = 0.37$ ) as well as in the dorsal midbrain (co:  $0.0144 \pm 0.0005$  nuclei/ $\mu\text{m}^2$ ; *Wnt1Cre-Smad4*:  $0.0141 \pm 0.0005$  nuclei/ $\mu\text{m}^2$ ;  $n = 4$ ;  $P = 0.75$ ).

### ***Increased Proliferation in the Dorsal and Ventral Midbrain Upon Loss of Smad4***

Immunohistochemical analysis revealed that the vast majority of the cells found in the expanding midbrain tissue of *Smad4*

cko embryos were undifferentiated and expressed the NSC marker Sox2, while only few Dcx-positive early neurons were detectable (Fig. 1E,F) at E12.5. To address whether the apparent increase in the number of NSCs was due to a change in proliferation, we quantified the mitotic index (number of cells in M-phase) in *Smad4* cko and control embryos. At E11.5, that is, before massive morphological changes were detectable (Fig. 1B), the number of cells in M-phase assessed by pHH3 staining was increased by 53.1% in the dorsal midbrain and even by 100.1% in the ventral midbrain (Fig. 2A,B), revealing an increase in the absolute numbers of mitotic cells in *Wnt1Cre-Smad4* mutants. Moreover, quantification of pHH3-positive cells amongst Sox2-positive NSCs showed an increased mitotic rate in the *Wnt1Cre-Smad4* mutant midbrain (Fig. 2A,C). As an amplification step for neuronal progeny during development, apically dividing NSCs can give rise to nonapically dividing basal progenitors that in turn divide symmetrically to produce 2 neurons (Haubensak et al. 2004; Miyata et al. 2004; Noctor et al. 2004). However, no significant difference in the fraction of basally dividing pHH3-positive cells between control and mutant midbrains at E11.5 was detectable (co:  $1.00 \pm 0.25$ ; *Wnt1Cre-Smad4*:  $1.28 \pm 0.15$ ;  $n = 4$ ;  $P = 0.37$ ), indicating that apically dividing stem cells lacking *Smad4* produced basal progenitors with normal frequency.

Complementary to the proliferation phenotype, quantification of early differentiating Dcx-expressing cells at E11.5 revealed that in the ventral as well as in the dorsal midbrain, the number of early neurons was markedly reduced (Fig. 2A,D). In agreement with earlier findings showing that TGF $\beta$ 2 and TGF $\beta$ 3 are required for dopaminergic neurogenesis in the ventral midbrain (Roussa et al. 2006), a specific reduction of tyrosine hydroxylase (TH)-positive dopaminergic neurons in the *Wnt1Cre-Smad4* mutant ventral midbrain was observed (Supplementary Fig. 2). These data show that rather than to produce differentiating progeny, NSCs in the *Smad4*-deficient midbrain divide to expand the pool of progenitor cells.

The increase in the number of proliferating cells concomitant with a decrease in the number of differentiated cells might be due to *Smad4*-deficient NSCs choosing to stay in, rather than to exit, the cell cycle. To address this, we pulse-labeled the embryos with the thymidine analog BrdU 20 h before analysis, followed by an immunostaining for the cell cycle marker Ki67 at the time point of analysis. In such an assay, cells having left the cell cycle at the time point of analysis are BrdU positive, but do not express the cell cycle marker Ki67. Therefore, the number of BrdU-positive but Ki67-negative cells gives a relative measure for the frequency of cells exiting the cell cycle. At E11.5, before major morphological changes were apparent in *Smad4* cko embryos, a massive decrease in cell cycle exit was detectable in both the mutant dorsal (Fig. 2E,F) and ventral midbrain (Fig. 2F), indicating a crucial role of Smad4-dependent signaling in cell cycle exit control. Moreover, quantification of the proportion of neurons formed in this 20 h window (Dcx-positive BrdU-positive/Dcx-positive cells) did not show any statistically significant difference neither in the dorsal (co:  $0.24 \pm 0.03$ ; *Wnt1Cre-Smad4*:  $0.26 \pm 0.01$ ;  $n = 3$ ;  $P = 0.55$ ) nor in the ventral midbrain (co:  $0.12 \pm 0.01$ ; *Wnt1Cre-Smad4*:  $0.13 \pm 0.01$ ;  $n = 3$ ;  $P = 0.57$ ). This finding reveals that cells exiting the cell cycle adopt a neuronal fate at a similar rate in *Wnt1Cre-Smad4* mutants as in controls.

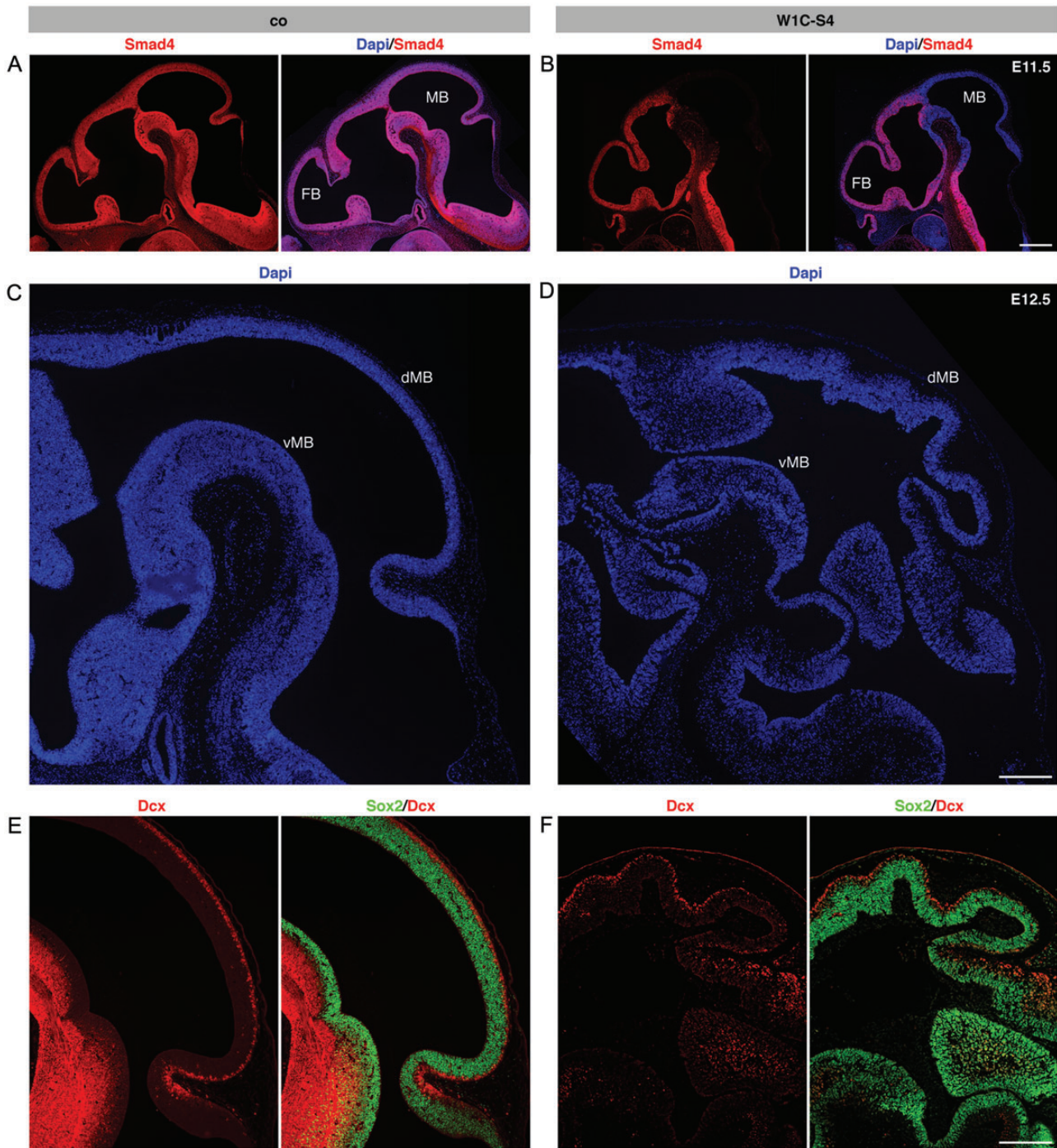


**Figure 1.** Loss of *Smad4* results in lateral expansion of the neuroepithelium in the dorsal and ventral midbrain. (A) At E11.5, *Smad4* is ubiquitously expressed in the entire CNS. *Wnt1-Cre*-driven recombination results in loss of *Smad4* in the midbrain at E11.5 (B) and subsequently to a massive lateral expansion of the neuroepithelium at E12.5 (C, D). Staining for *Sox2* and *Dcx* demonstrates that the expanding tissue at E12.5 is mainly composed of undifferentiated *Sox2*-positive precursor cells while only a few differentiated *Dcx*-positive neurons are detectable (E, F). W1C-S4: *Wnt1Cre-Smad4* mutants. FB, forebrain; MB, midbrain; dMB, dorsal midbrain; vMB, ventral midbrain. Scale bars: (B, D, F) 200  $\mu$ m.

#### ***Smad4* Deletion has No Effect on NSCs in the Forebrain**

Previously, loss of TGF $\beta$  signaling by *Tgfr2* inactivation did not elicit an overt phenotype in NSCs of the developing dorsal forebrain, unlike in the dorsal midbrain (Falk et al. 2008). These findings either suggest that compensatory mechanisms act in the forebrain or point to a brain area-restricted role of TGF $\beta$  signaling during CNS development. To address a

potential role of canonical TGF $\beta$  signaling in the dorsal forebrain, we conditionally deleted *Smad4* in this area using the *Emx1Cre* knock-in line (Gorski et al. 2002). In this line, Cre protein starts to be expressed at around E9.5, before the onset of forebrain neurogenesis (Cappello et al. 2006). In *Emx1Cre-Smad4* embryos, the *Smad4* protein was undetectable in nearly all cells of the forebrain at E14.5 (Supplementary

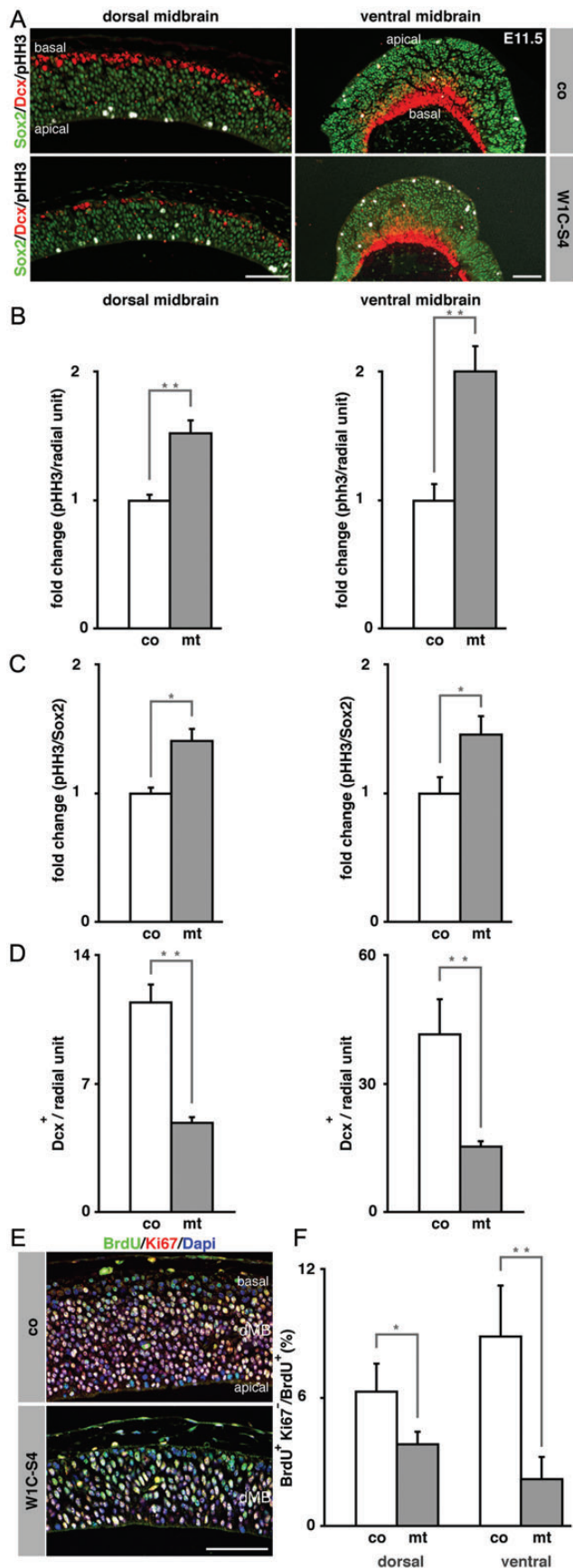


**Figure 2.** Increased proliferation, decreased differentiation, and reduced cell cycle exit are the cellular effects leading to midbrain enlargement in *Smad4* mutants. (A, B) At

Fig. 3A), but was expressed in ventral structures (Supplementary Fig. 3A, asterisk). Despite an almost complete loss of Smad4 protein, and hence a complete loss of any Smad4-dependent signaling, no effect on NSCs was observable in *Smad4*-deficient forebrains in vivo. Whole-brain preparations visualizing recombination by means of the Rosa26 Cre reporter (Soriano 1999) showed no expansion of recombined tissue, neither at E16.5 nor at E18.5 (Supplementary Fig. 3B,C). In addition, immunohistochemistry on E18.5 coronal sections revealed no expansion of proliferative neuroepithelial structures (Supplementary Fig. 3D,E). Accordingly, there was also no evident change in the number of differentiating neurons (Supplementary Fig. 3E). Mutant mice were born at the expected Mendelian ratio, excluding the possibility that affected embryos die during embryonic development and, therefore, might have been missed in the analysis. These unexpected findings reveal that the Smad4-dependent canonical TGFβ superfamily pathway is not required by NSCs during the development of the forebrain in vivo.

#### Early During Cortical Development, Proliferation and Differentiation of NSCs are Unaffected by Ablation of *Smad4* and *Trim33*

A molecule implicated in TGFβ signaling and, as we hypothesized, might also be important in the process of area-specific control of NSCs by this signaling pathway, is *Trim33* (also known as *Tif1γ*, *Ectodermin* or *moonshine*). In hematopoietic stem cells, *Trim33* physically interacts with receptor-activated Smad2/3 in competition with Smad4 and thereby regulates erythrocyte differentiation, whereas the complex Smad4/pSmad2/3 regulates proliferation in these cells (He et al. 2006). Another report showed that *Trim33* is a monoubiquitin ligase, ubiquitinating Smad4 in the nucleus and thereby terminating TGFβ signal activity (Dupont et al. 2005). Thus, the molecular function of *Trim33* remains controversial. Yet the model, in which *Trim33* can propagate Smad2/3 signaling similar to Smad4 (He et al. 2006), offers the possibility that in the dorsal forebrain *Trim33* might compensate for the loss of Smad4. In contrast, should the ubiquitination model (Dupont et al. 2005) hold true for the murine dorsal forebrain, no effect upon loss of *Trim33* would be expected.

The generation of a floxed conditional allele for *Trim33* (Kim and Kaartinen 2008), leading to the loss of *Trim33*

E11.5, before the massive morphological changes apparent at E12.5 develop, an increase in the number of mitotic cells (pHH3-positive) per total cell number is detectable in the dorsal (co: 1.00 ± 0.04; Wnt1Cre-Smad4: 1.53 ± 0.09; n = 4) as well as in the ventral midbrain (co: 1.00 ± 0.14; Wnt1Cre-Smad4: 2.00 ± 0.20; n = 4). (A, C) At the same time point, a relative increase in the number of mitotic cells per Sox2-positive cells is measurable in the dorsal (co: 1.00 ± 0.03; Wnt1Cre-Smad4: 1.41 ± 0.09; n = 4) and in the ventral midbrain (co: 1.00 ± 0.13; Wnt1Cre-Smad4: 1.46 ± 0.14; n = 4). (A, D) Concomitant with the increase in proliferative cells, less early differentiating neurons are detectable in the entire midbrain as assessed by quantification of Dcx-positive cells per radial unit of 100 μm (dorsal midbrain: co: 11.46 ± 0.95; Wnt1Cre-Smad4: 4.97 ± 0.18; n = 3) (ventral midbrain: co: 41.79 ± 7.58; Wnt1Cre-Smad4: 15.62 ± 0.81; n = 3). (E, F) Cell cycle exit was addressed by determining the fraction of cells that incorporated BrdU (BrdU-positive), when pulsed 20 h before analysis but were not proliferating (Ki67-negative) anymore at the time point of analysis as illustrated for the dorsal midbrain in (E). A severe reduction in cell cycle exit was observed at E11.5 in the dorsal midbrain (co: 6.79 ± 1.49%; Wnt1Cre-Smad4: 3.82 ± 0.49%, n = 3) as well as in the ventral midbrain (co: 8.87 ± 2.47%; Wnt1Cre-Smad4: 2.17 ± 1.06%; n = 3). W1C-S4: Wnt1Cre-Smad4 mutants. \*P < 0.05; \*\*P < 0.01. Scale bars (A, E): 100 μm.

protein after recombination (Supplementary Fig. S4), made it possible to address the question of whether *Trim33* and *Smad4* have redundant function in the developing cortex. Conditional double knockout embryos with both genes *Smad4* and *Trim33* mutated in the developing forebrain were produced using the *Emx1Cre* line (Gorski et al. 2002). At E13.5, that is, a day later than the stage when in the midbrain ablation of *Smad4* alone led to the dramatic horizontal expansion of the neuroepithelium, the forebrain did not show any apparent alteration in respect to differentiation and proliferation (Fig. 3A, C). The earliest neurons born are the cortical hem-derived Reelin-expressing Cajal-Retzius cells in layer 1 of the cortex (Yoshida et al. 2006). No differences in terms of numbers, density, or localization of these neurons were observed between conditional double mutant animals and control littermates (Fig. 3A). Furthermore, at E13.5, no alteration in the number or location of early born *Tbr1*-expressing cells was detectable in the cortex of *Emx1Cre-Smad4-Trim33* double conditional knockout embryos (Fig. 3A,B). Determining the total amount of dividing cells (Fig. 3C,D) as well as the mitotic index in the Sox2-positive apical progenitor population (Fig. 3C,E) and in the *Tbr2*-positive basal progenitor population (Fig. 3C,F) revealed that there was no difference in proliferation at this stage. These findings reveal that during early stages of cortical development *Trim33* and *Smad4* are neither required for proper NSCs function nor do they compensate for each other.

#### Delayed Progression of NSCs From Producing Deep Layer Neurons to Upper Layer Neurons

Normally at E17.5, NSCs in the developing cortex have undergone a transition to produce late born upper layer neurons expressing *Cux1* and *Satb2* and have stopped generating deep layer neurons positive for *Tbr1* (Fig. 4). Similarly, single conditional knockout embryos (*Emx1Cre-Smad4* and *Emx1Cre-Trim33*, respectively) displayed no overt changes in the formation of deep and upper layer neurons (Fig. 4). However, in *Smad4-Trim33* conditional double mutants, quantification of *Tbr1* expressing cells at E17.5 revealed a 46.2% increase in the number of deep layer neurons when compared with control littermates (Fig. 4A,B). While there was a prominent cell layer between Reelin-expressing layer 1 neurons and *Tbr1*-positive deep layer neurons in control and single cko animals, this zone was completely missing in *Emx1Cre-Smad4-Trim33* double mutant animals (Fig. 4A). Intriguingly, this region corresponds to the area normally populated by late born upper layer neurons. Indeed, staining for *Cux1* and *Satb2* revealed virtual absence of upper layer neurons in double mutant embryos at E17.5, in contrast to control and single mutant littermates (Fig. 4C,D,E,F). The number of apoptotic nuclei found in the brain at this stage was not changed (data not shown), speaking against the possibility that upper layer neurons are generated in *Emx1Cre-Smad4-Trim33* double mutants but die once formed. Thus, *Smad4* and *Trim33* exert redundant functions in the temporal control of cortical neurogenesis, each compensating for the loss of the other one in single mutants. Cortical NSCs lacking both *Smad4* and *Trim33* fail to produce upper layer neurons at E17.5 and apparently continue to produce deep layer neurons. However, analysis of *Cux1* and *Satb2* expression at postnatal day 0 (P0) revealed that upper layer neurons were eventually produced in *Emx1Cre-Smad4-Trim33*

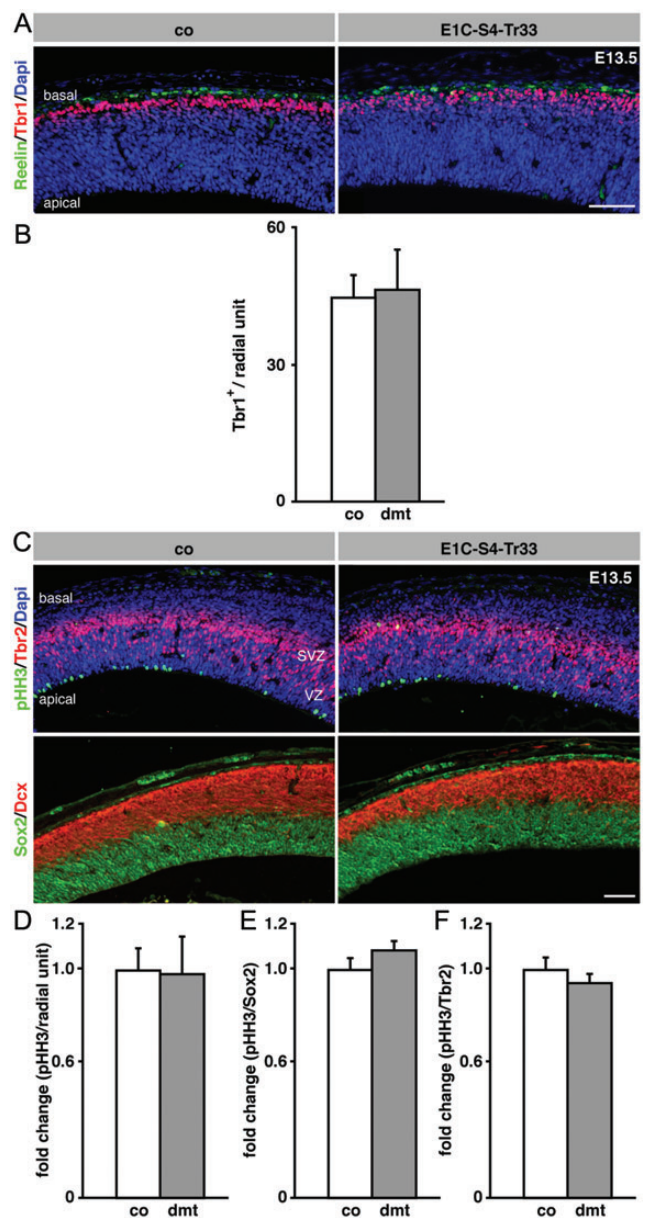


**Figure 3.** Normal proliferation and differentiation in the dorsal forebrain at midneurogenic stages upon concomitant deletion of *Smad4* and *Trim33*. (A, B) *Emx1Cre*-mediated conditional ablation of *Smad4* and *Trim33* in the dorsal forebrain has neither an effect on the production of the earliest formed neurons, the Reelin-positive Cajal-Retzius cells, nor on *Tbr1*-positive cells at E13.5 (co: 45.28 ± 4.53; *Emx1Cre-Smad4-Trim33*: 46.91 ± 8.68; *n* = 3). (C, D) At the same developmental stage, the total number of mitotic cells (pHH3-positive) is unchanged upon loss of *Smad4* and *Trim33* (co: 1.00 ± 0.09; *Emx1Cre-Smad4-Trim33*: 0.98 ± 0.16; *n* = 3). (C, E, F) Moreover, no change in the number of dividing cells in the Sox2-positive population (co: 1.00 ± 0.05; *Emx1Cre-Smad4-Trim33*: 1.09 ± 0.04; *n* = 3) as well as in the *Tbr2*-positive population (co: 1.00 ± 0.05; *Emx1Cre-Smad4-Trim33*: 0.94 ± 0.04; *n* = 3) was detectable. Radial unit: 100  $\mu$ m. E1C-S4-Tr33, *Emx1Cre-Smad4-Trim33* double mutants; dmt, double mutant. Scale bars: 100  $\mu$ m.

animals. At P0, *Cux1*-positive and *Satb2*-positive neurons were detectable in the outer cortical layers, although the number of these neuronal subtypes was still significantly reduced when compared with control embryos while the number of *Tbr1*-positive deep layer neurons was found to be increased (Fig. 5A,B). The reduced ratio of upper to deeper layer neurons (*Cux1* to *Tbr1*) in *Emx1Cre-Smad4-Trim33* double

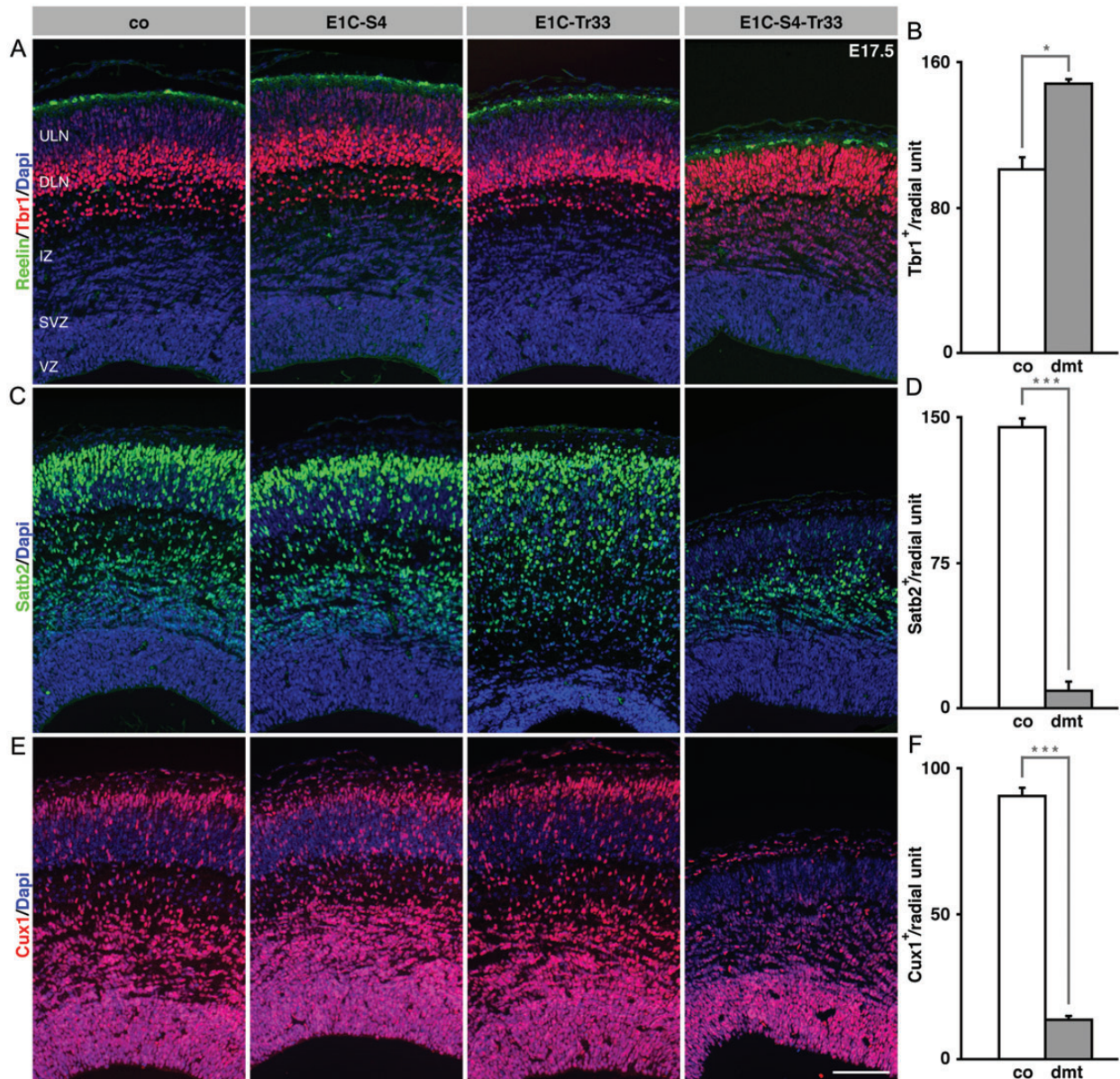


**Figure 4.** Excessive numbers of deep layer neurons and reduced numbers of upper layer neurons in the *Smad4-Trim33* double mutant forebrain. (A, B) Immunohistochemical analysis and quantification of Tbr1 expressing neurons at E17.5 revealed a 46% increase of deep layer neurons upon concomitant ablation of *Smad4* and *Trim33* in the dorsal forebrain (co:  $101.36 \pm 5.87$ ; Emx1Cre-Smad4-Trim33:  $148.20 \pm 1.47$ ;  $n = 3$ ). Note the absence of a specific layer between Reelin-positive (green) and Tbr1-positive (red) cells in Emx1Cre-Smad4-Trim33 double mutants normally populated by upper layer neurons (arrows). Indeed, a drastic reduction in the number of upper layer neurons found in the cortical plate of *Smad4-Trim33*-deficient dorsal forebrain is detectable as shown by staining and quantification for (C, D) Satb2 (co:  $146.94 \pm 3.77$ ; Emx1Cre-Smad4-Trim33:  $11.09 \pm 3.71$ ;  $n = 3$ ) and (E, F) Cux1 (co:  $90.90 \pm 2.41$ ; Emx1Cre-Smad4-Trim33:  $13.60 \pm 0.31$ ;  $n = 3$ ). E1C-S4, Emx1Cre-Smad4 mutants; E1C-Tr33, Emx1Cre-Trim33 mutants; E1C-S4-Tr33, Emx1Cre-Smad4-Trim33 double mutants. Radial unit: 100  $\mu\text{m}$ . dmt, double mutant. \* $P < 0.05$ ; \*\*\* $P < 0.001$ . VZ, ventricular zone; SVZ, subventricular zone; IZ, intermediate zone; DLN, deep layer neuron; ULN, upper layer neurons. Scale bars: 150  $\mu\text{m}$ .

mutant animals strengthens the finding of a delayed switch to upper layer neurons production (Fig. 5C). Taken together, these data show that in the developing cortex TGF $\beta$  signaling is not required for the actual specification of upper layer neurons. Rather, signaling via both Smad4 and Trim33 regulates the proper timing of the switch from producing early born deep layer neurons to later born upper layer neurons.

#### Signaling via Smad4 and Trim33 Controls the Timely Specification of Glial Precursors

After the temporally controlled inside out generation of the different neuronal layers of the cortex, the progenitors in the

ventricular zone of the mammalian dorsal forebrain proceed with the production of glial cells. In the dorsal forebrain of mice, this transition happens around E18 when the first differentiated glial cells are detectable (Miller and Gauthier 2007). Given the delay in the production of later born upper layer neurons in the combined *Emx1Cre-Smad4-Trim33* knockout, we tested whether the neurogenic-to-gliogenic switch in NSCs is also affected. First we examined Olig2, a molecule expressed by glial progenitors particularly in the ganglionic eminences but at later stages also present in the ventricular zone (VZ) of the dorsal telencephalon. In *Smad4-Trim33* deficient E17.5 embryos, almost no Olig2-positive cells were detectable in the

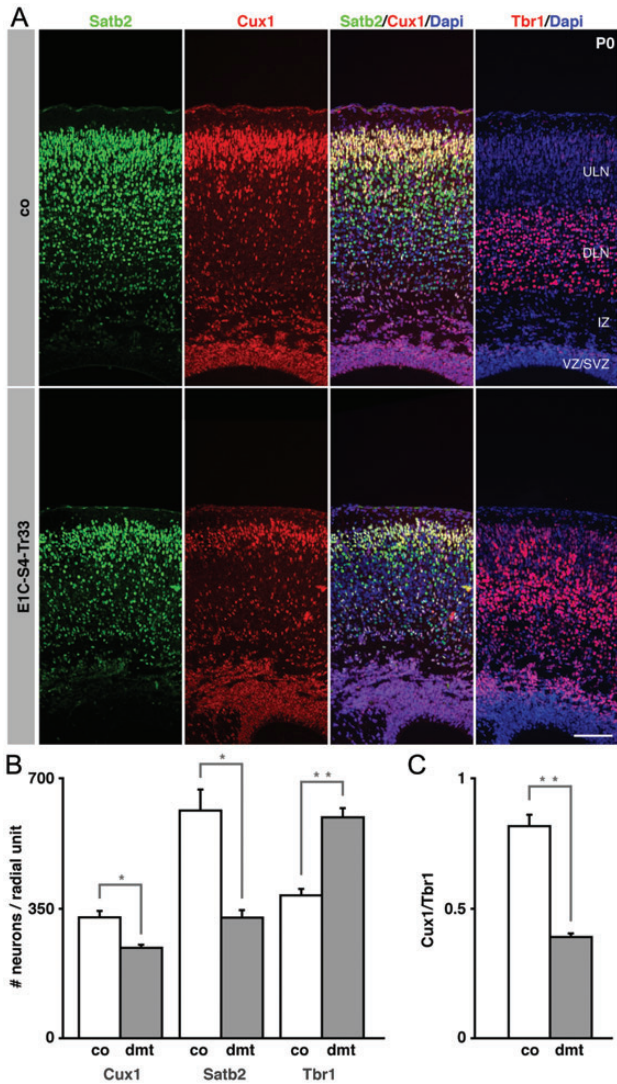


**Figure 5.** Deletion of *Smad4* and *Trim33* results in delayed formation of upper layer neurons. (A, B) At P0, *Satb2*-positive as well as *Cux1*-positive upper layer neurons are detectable in the *Smad4-Trim33*-mutant dorsal forebrain, uncovering a delay rather than a complete block in the production of these specific cells. *Cux1* (co: 330.92 ± 11.70; *Emx1Cre-Smad4-Trim33*: 247.39 ± 4.27; *n* = 3), *Satb2* (co: 620.41 ± 54.53; *Emx1Cre-Smad4-Trim33*: 329.33 ± 17.83; *n* = 3), *Tbr1* (co: 392.18 ± 12.87; *Emx1Cre-Smad4-Trim33*: 609.98 ± 18.51; *n* = 3). (C) The ratio of upper layer neurons (*Cux1*+) to deep layer neurons (*Tbr1*+) shows a clear reduction in the double mutant brain (co: 0.84 ± 0.03; *Emx1Cre-Smad4-Trim33*: 0.41 ± 0.01; *n* = 3). E1C-S4-Tr33, *Emx1Cre-Smad4-Trim33* double mutants. Radial unit: 100 μm. dmt, double mutant. \**P* < 0.05. VZ, ventricular zone; SVZ, subventricular zone; IZ, intermediate zone; DLN, deep layer neuron; ULN, upper layer neurons. Scale bars: 100 μm.

dorsal telencephalic VZ (Fig. 6A, arrows), while some *Olig2*-positive cells, most probably derived from the ganglionic eminence, were detectable in the cortex outside of the proliferative zone (Fig. 6A, arrowheads). Quantification of *Olig2*-positive cells in the VZ disclosed an 83.4% reduction in the number of *Olig2*-positive cells, suggesting that precursor cells in the dorsal telencephalon failed to acquire glial features at this stage (Fig. 6A, B). In contrast, in the nonrecombined ventral part of the telencephalon, *Olig2* was readily detectable (Fig. 6A, asterisk). Moreover, we found less glial-fibrillary acidic protein (GFAP)-positive astrocytes in *Emx1Cre-Smad4-Trim33* kco cortices at P0 (Fig. 6C), further strengthening the finding that the neurogenic-to-gliogenic switch in NSCs is

impaired in double conditional knockout embryos. Therefore, *Smad4* and *Trim33* not only control the temporal maturation of neurogenic NSCs (Figs 4, 5), but also act in concert to regulate the timely production of glia from cortical NSCs (Fig. 6).

### Increased Proliferation and Reduced Cell Cycle Exit in *Smad4* and *Trim33* Double Deficient Cortex

The failure of NSCs in *Emx1Cre-Smad4-Trim33* kco embryos to produce appropriate numbers of particular neuronal subtypes and glia at E17.5 might be linked to deregulated cell cycle progression at this developmental stage. Similarly, in the *Smad4*-deficient midbrain, decrease of neurogenesis is associated with increased proliferation and decreased cell cycle exit. To address this hypothesis, we first determined the number of mitotic cells in control and *Smad4-Trim33* double mutant brains by analyzing pHH3 expression at E17.5. Strikingly, a 70.7% increase in the number of mitotic cells was detectable in *Emx1Cre-Smad4-Trim33* forebrain tissue when compared with cortices of control littermates (Fig. 7A,B). Moreover, quantification of pHH3-positive cells amongst all *Sox2*-positive NSC revealed an increased mitotic rate in these progenitor cells at E17.5 (Fig. 7A,C). The altered proliferation in the *Smad4-Trim33*-deficient forebrain was confirmed by investigating the degree of cell cycle exit of proliferative cells. This was achieved by i.p. injection of pregnant females with BrdU 20 h before analysis, combined with staining for the proliferation marker Ki67 at the time point of analysis (Fig. 7D). In control forebrain at E17.5, many proliferative cells as well as cells having exited the cell cycle were present outside the ventricular zone (VZ), seemingly migrating through the intermediate zone (IZ) before differentiation (Fig. 7D). In the *Smad4-Trim33* deficient dorsal forebrain, however, these cell populations were mostly missing and proliferation was almost exclusively restricted to the VZ and subventricular zone (SVZ). Quantification of the number of BrdU-positive/Ki67-positive cells confirmed the increase in proliferative cells in the VZ/SVZ (Fig. 7E). Importantly, there was a 71.9% drop in the overall number of BrdU-positive/Ki67-negative cells per total number of BrdU-positive cells in the *Emx1Cre-Smad4-Trim33* double mutant cortex, reflecting a drastic reduction in the cell cycle exit rate (Fig. 7F). Therefore, the combined inactivation of *Smad4* and *Trim33* in the dorsal forebrain leads to an increase of proliferating cells in the VZ due to reduced cell cycle exit. Strikingly, this effect is stage-specific as the simultaneous lack of *Smad4* and *Trim33* did not influence cortical precursor cells early in development but only affected a particular step in their maturation process, namely, during late neurogenic and gliogenic phases.

### Discussion

During CNS development, different regions of the neural tube have to grow to a specific extent in a given time frame. From a rather small starting population of NSCs undergoing a series of symmetric divisions, a stem cell pool has to be established that is large enough to be able to produce all the neurons and glial cells needed in the mature nervous system. Subsequently, at the right time and with the appropriate frequency, the NSCs have to switch from symmetric proliferative divisions to the production of neurons and eventually glial cells to ensure the proper balance between the number of precursor cells and the



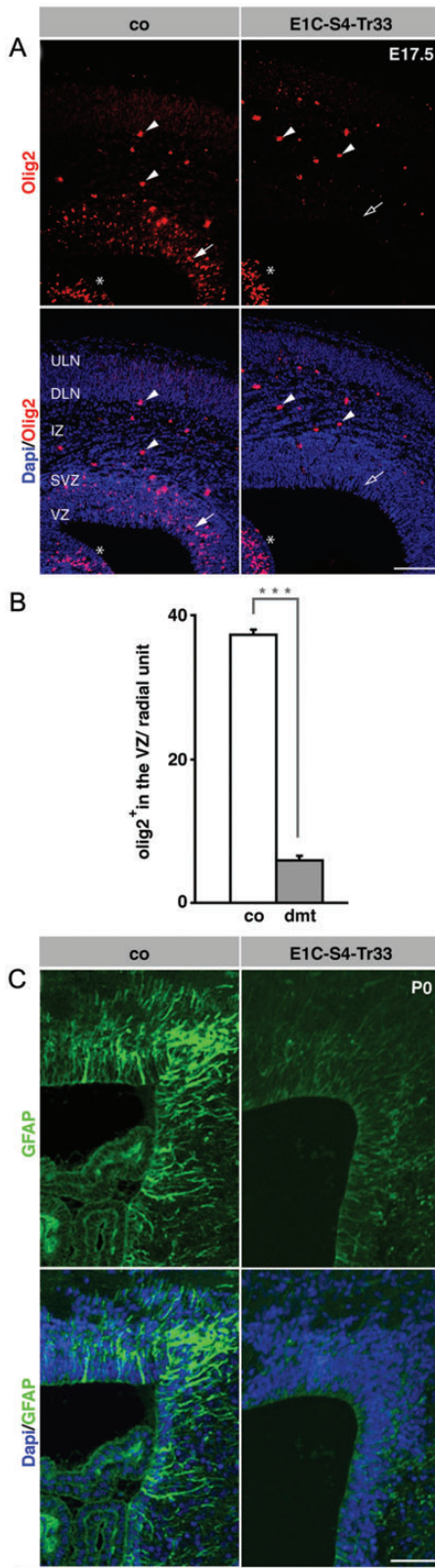


**Figure 6.** The switch from making neurons to the production of glia in the dorsal forebrain is controlled by *Smad4* and *Trim33*. (A, B) Staining for Olig2 at E17.5 discloses the presence of glial progenitors in the ventricular zone of control animals (arrows) at this stage. However, these cells are lost upon deletion of *Smad4* and *Trim33* in the dorsal forebrain (open arrow) (co:  $37.55 \pm 0.36$ ; *Emx1Cre-Smad4-Trim33*:  $6.21 \pm 0.52$ ;  $n = 3$ ). Note the normal expression of Olig2 in the non-recombined ventral forebrain (asterisk) as well as the presence of

amount of differentiated offspring (Rakic 1995, 2009). Given the many different regions in the CNS, it is conceivable that the accurate regulation of these processes involves area-specific mechanisms (Falk and Sommer 2009). We reveal signaling by the TGF $\beta$  superfamily of cytokines to be a central knot in the regulatory networks controlling growth of the NSC pool and the timely generation of differentiated progeny in distinct brain regions. Thereby, different regions in the developing CNS make use of distinct branches of the TGF $\beta$  signaling pathway. NSCs in the dorsal midbrain require signaling via *Tgfr2* to control stem cell self-renewal (Falk et al. 2008), while in the ventral midbrain, a different arm of the pathway signaling via *Smad4* (Fig. 7G), but not via *Tgfr2*, is responsible to control similar aspects of development. In the dorsal forebrain, on the other hand, *Smad4* and *Trim33* act together to control proliferation and differentiation of NSCs. In this CNS area, *Smad4* and *Trim33* regulate the temporal progression of NSCs and control a specific maturation step during the neurogenic phase as well as the transition from neurogenic to gliogenic differentiation (Fig. 7H).

### *Smad4* and *Trim33* act Functionally Redundant

How exactly *Smad4* and *Trim33* exert their activities in the developing forebrain remains to be elucidated. Indeed, the molecular function of *Trim33* has been controversial (Dupont et al. 2005; He et al. 2006; Dupont et al. 2009; Morsut et al. 2010; Xi et al. 2011). On the one hand, *Trim33* and *Smad4* have been reported to act in parallel pathways, both competing for the binding to R-Smads in hematopoietic stem cells (He et al. 2006). In these cells, differential R-Smad-binding by either *Trim33* or *Smad4* leads to differential signaling readout, promoting either differentiation or proliferation. According to another study, *Trim33* acts directly on *Smad4* by physical interaction with and ubiquitination of *Smad4*, leading to inhibition of *Smad4*-dependent signaling (Dupont et al. 2005). Conceivably, the mode of *Trim33* action might be context- and cell type-specific. At least in the developing dorsal forebrain, however, our genetic approach revealing functionally redundant action of *Smad4* and *Trim33* excludes the model, according to which *Trim33* is a negative regulator of *Smad4*. Ablation of *Smad4* alone did not have any overt effect on cortical NSCs. Therefore, in these cells, we would not expect any effect upon conditional deletion of both *Smad4* and *Trim33*, if the function of *Trim33* were to counteract *Smad4* by terminating its response to a cytokine stimulus. However, our data do not necessarily mean that in the developing forebrain *Trim33* binds to pSmads and acts as a co-Smad, as shown for the hematopoietic system. For instance, *Trim33* on its own might regulate similar processes as activated by the target genes of the *Smad4* pathway, or *Trim33* might control similar target genes independently of the *Smad4* pathway.

### Area-Specific Differences in the Control of NSC Proliferation vs. Differentiation

Signaling by TGF $\beta$  superfamily members, especially BMPs, is responsible for regionalization events in the early developing

Olig2-positive cells in the intermediated zone most probably derived from ventral structures (arrowheads). (C) Expression of GFAP was strongly reduced in *Emx1Cre-Smad4-Trim33* double mutants. E1C-S4-Tr33, *Emx1Cre-Smad4-Trim33* double mutants. Radial unit: 100  $\mu$ m. dmt, double mutant. \*\*\* $P < 0.001$ . VZ, ventricular zone; SVZ, subventricular zone; IZ, intermediate zone; DLN, deep layer neuron; ULN, upper layer neurons. Scale bars: 100  $\mu$ m.

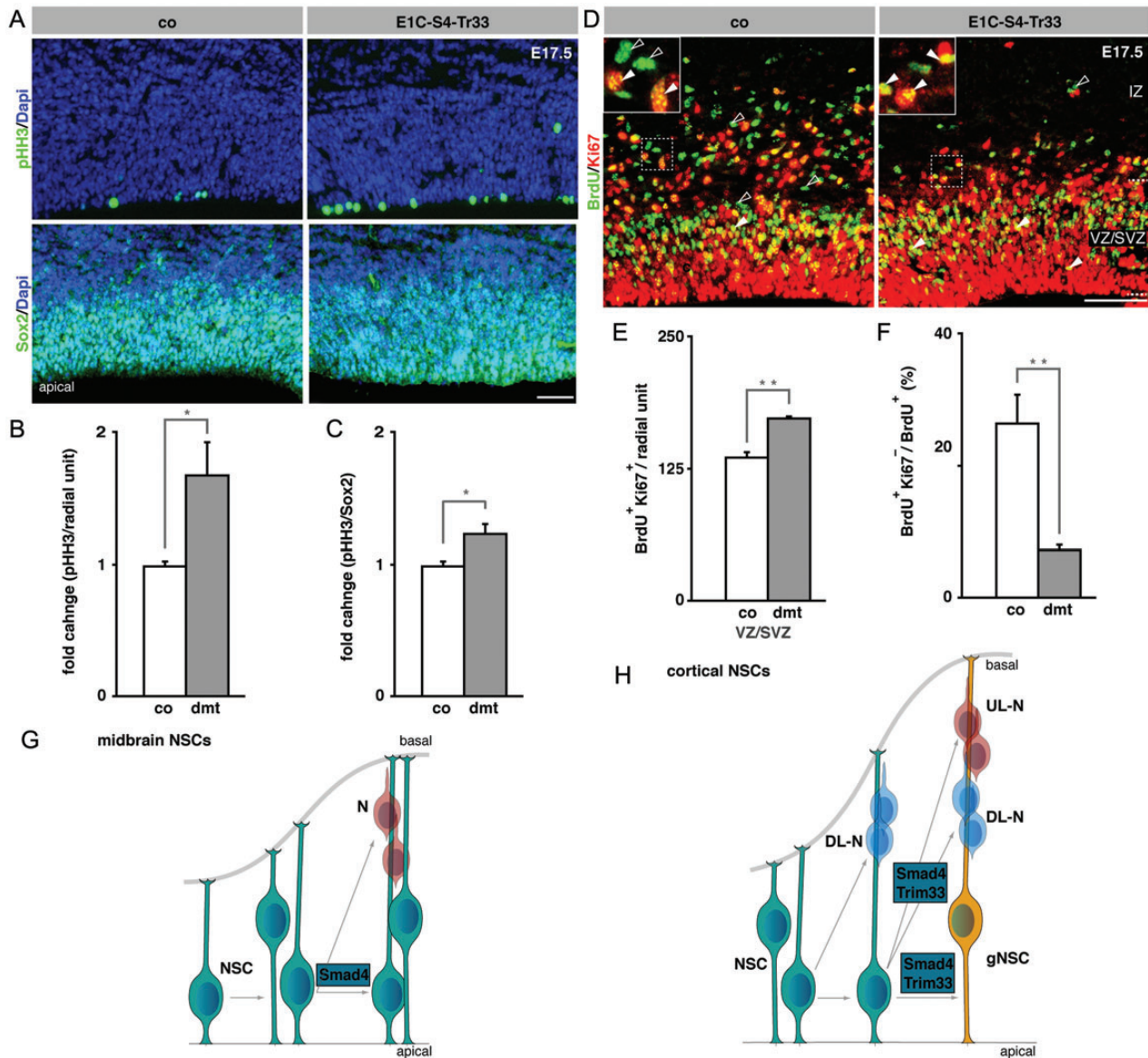


**Figure 7.** Increased proliferation and decreased cell cycle exit in the *Smad4-Trim33* double mutants at E17.5 as shown by staining and quantification of pHH3-positive cells per radial unit (co:  $1.00 \pm 0.05$ ; Emx1Cre-*Smad4-Trim33*:  $1.71 \pm 0.24$ ;  $n = 3$ ) and of pHH3-positive cells in the Sox2-positive population (co:  $1.00 \pm 0.04$ ; Emx1Cre-*Smad4-Trim33*:  $1.25 \pm 0.07$ ;  $n = 3$ ) (C). (D) To further analyze proliferation and cell cycle exit, embryos were pulsed once with BrdU and examined 20 h later. (E) Quantification of cells positive for both BrdU and Ki67 in the VZ/SVZ (arrowheads) further strengthened the finding of increased proliferation in the double mutants (co:  $137.54 \pm 3.57$ ; Emx1Cre-*Smad4-Trim33*:  $173.37 \pm 6.59$ ;  $n = 3$ ). (F) To determine the fraction of cells exiting the cell cycle in this 20-h window, the number of BrdU-positive but Ki67-negative cells (open arrowheads) per total number of BrdU-positive cells was quantified. A strong reduction in cell cycle exit could be observed in *Smad4-Trim33* deficient brains (co:  $26.64 \pm 4.02\%$ ; Emx1Cre-*Smad4-Trim33*:  $7.47 \pm 0.68\%$ ;  $n = 3$ ). (G) Model illustrating the role of Smad4 in the regulation of the balance between proliferation and differentiation of midbrain NSCs. (H) Schematic representation of the role of Smad4 and Trim33 in controlling the temporal maturation of cortical NSCs. Together Smad4 and Trim33 are required to govern the switch from deep layer neurons (DLN) to upper layer neurons (ULN) as well as for acquiring of more glial features by the NSCs (gNSC). E1C-S4-Tr33: Emx1Cre-*Smad4-Trim33* double mutants. VZ/SVZ, ventricular zone/subventricular zone. IZ, intermediated zone. Radial unit: 100  $\mu\text{m}$ . dmt, double mutant. \* $P < 0.05$ ; \*\* $P < 0.01$ . Scale bars: 100  $\mu\text{m}$ .

CNS specifying the different areas in the proto-map (Rakic 1988). Specifically, it was shown that BMP signaling via *Bmpr1a* is only crucial for the specification of the most dorsomedial structure in the forebrain, the choroid plexus (Hebert et al. 2002). In vitro, *Bmp4* is sufficient to induce features of this midline structure like expression of *Msx1* and inhibition of proliferation (Furuta et al. 1997). However, In vivo, although highly expressed in medial structures, genetic deletion of the ligand *Bmp4* did not evoke patterning defects in the developing forebrain (Hebert et al. 2003), disclosing that the ligand

*Bmp4* alone is not required for proper patterning of the forebrain and suggesting that other *Bmp* ligands might compensate for the loss of *Bmp4*. These data reveal that the readout of *Bmp* exposure is very area-specific in cortical structures. In this study, we show that different regions of the developing CNS have an area-specific requirement for the core signaling machinery of the TGF $\beta$  pathway composed of Smad4 and Trim33. In the midbrain, deletion of *Smad4* alone already had a drastic effect on NSC proliferation. Of note, massive expansion of the neuroepithelium was observed in both the dorsal

and ventral *Smad4* cko midbrain. This is in contrast to the *Tgfr2*-deficient midbrain, in which only dorsal but not ventral NSCs excessively proliferate (Falk et al. 2008). The most parsimonious explanation for these midbrain region-specific differences in TGF $\beta$  signaling is the differential but partially overlapping expression pattern of TGF $\beta$  family members, which could lead to local factor redundancy. During early brain development, TGF $\beta$  ligands are expressed in the choroid plexus and, as factors secreted into the cerebrospinal fluid, are thought to have the capacity for signal activation throughout the CNS neuroepithelium (Falk et al. 2008). In contrast, Activin $\beta$ B is expressed in the ventral midbrain and the dorsal forebrain but not in the dorsal midbrain (Feijen et al. 1994). As Activins and TGF $\beta$ s use distinct receptors but both activate canonical Smad-dependent signaling (Massague 2008), *Smad4*-deletion terminates signaling even in areas of potential factor redundancy. In the developing midbrain, this is exactly what we observed: *Smad4*-deficient ventral and dorsal midbrain NSCs display significantly reduced rates of cell cycle exit and differentiation and instead continue to proliferate. This leads to a drastic horizontal expansion and eventual undulation of the entire *Smad4*-mutant midbrain, revealing a crucial role of canonical TGF $\beta$  signaling in the control of size and shape of the developing midbrain.

In contrast, brain size control in the developing dorsal telencephalon involves more complex signaling and, consequently, inactivation of canonical TGF $\beta$  signaling by conditional *Smad4* deletion is not sufficient to alter forebrain NSC proliferation and cell cycle exit. As we show here, dorsal forebrain NSC behavior is only affected upon concomitant inactivation of *Smad4* and *Trim33*. However, differences in the growth requirements by midbrain and forebrain NSCs cannot simply be explained by the expression patterns of *Smad4* and *Trim33*, because both molecules are ubiquitously expressed in the entire developing CNS. A protein likely to be involved in the described area-specific control mechanisms is the forkhead transcription factor FoxG1. FoxG1 is specifically expressed in the forebrain where it regulates the differentiation of NSCs. In particular, FoxG1 suppresses early cortical cell fates, so that *FoxG1* null mutant embryos display an excess of the earliest born neurons, the Cajal-Retzius cells (Hanashima et al. 2004; Hanashima et al. 2007). Knockdown experiments in vivo revealed that the intrinsic timing mechanism regulating the maturation of NSCs is reset upon reduction of FoxG1 (Shen et al. 2006). Intriguingly, this resembles the phenotype we observed in *Emx1Cre-Smad4-Trim33* conditional double knock-out embryos, which also appears to be due to defective maturation of NSCs albeit at a later stage. In the context of TGF $\beta$  signaling, FoxG1 has been shown to interact with binding partners of Smads that are responsible to regulate transcription of TGF $\beta$  target genes (Dou et al. 2000). Moreover, FoxG1 binds to the FoxO/Smad complex and attenuates the expression of target genes, thereby granting resistance to TGF $\beta$ -mediated inhibition of proliferation in vitro (Seoane et al. 2004). Thus, *Smad4*-dependent signaling in the developing forebrain might be modulated by the activity of FoxG1.

Likely, control of NSCs by *Smad4* and *Trim33* also includes cell non-autonomous mechanisms. In the developing midbrain it was shown that signaling via *Tgfr2* is regulating the balance between proliferation and differentiation of NSCs by controlling the activation of the Wnt-pathway (Falk et al. 2008). Similarly, in the *Smad4* deficient midbrain, we also saw ectopic

expression of Wnt1 (data not shown). In the forebrain, however, Wnt1 expression appeared to be normal, indicating that other cell-extrinsic factors might contribute to NSC control in the developing forebrain.

### **Temporal Control of NSC Proliferation and Maturation**

During development, NSCs are subject to a maturation process that allows them to produce the right progeny at the right time (Falk and Sommer 2009; Okano and Temple 2009). One of the first steps in the temporal progression of NSCs is to switch from symmetric proliferative divisions early in development to asymmetric divisions whereby the first neurons are produced. In the developing forebrain, NSCs further mature to produce distinct cortical neurons in a temporally controlled manner, with deep layer neuron generation preceding upper layer neuron generation. A subsequent maturation step allows NSCs to switch from neurogenesis to gliogenesis. This temporal sequence is regulated by cell-intrinsic control mechanisms such as mediated by Ezh2, an essential component of the Polycomb complex. When ablated during cortical development, the temporal progression of *Ezh2*-deficient NSCs is accelerated, resulting in precocious generation of upper layer neurons and glia (Hirabayashi et al. 2009). Such intrinsic cues are modulated by extrinsic signals including, for instance, Notch ligands or the cytokine cardiotrophin-1 that confer glial potential in NSCs after completion of neurogenesis (Barnabe-Heider et al. 2005; Nami-hira et al. 2009). Likewise, FGF9 and NT3 regulate the switch from deep to upper layer neuron generation (Seuntjens et al. 2009). This latter process involves the Smad-interacting protein Sip1 that regulates the timely production of appropriate numbers of upper layer neurons by controlling FGF9 and NT3 expression. Interestingly, deletion of *Sip1* in the cortex had the opposite phenotype than what we found upon concomitant ablation of *Smad4* and *Trim33*. *Emx1Cre-Smad4-Trim33* knock-out embryos displayed excess deep layer neurons, delayed and reduced formation of upper layer neurons, and subsequently an impaired production of glial cells. In contrast, similar to the ablation of *Ezh2*, conditional deletion of *Sip1* induced precocious production of upper layer neurons at the expense of deep layer neurons as well as premature production of glial progeny (Seuntjens et al. 2009). Whether Ezh2, Sip1, and *Smad4/Trim33* independently control the timely generation of cortical neurons and glia or whether these molecules form part of a common regulatory knot controlling opposite effects in NSCs remains to be elucidated.

In addition to preventing acquisition of late cortical fates, ablation of *Smad4* and *Trim33* together led to increased proliferation and reduced cell cycle exit at the stage of late neuron production, but not at the time of early neurogenesis. This stage-specific function of *Smad4/Trim33* is possibly again associated with signal modulation by FoxG1 at early stages of cortical development. Indeed, only young NSCs, but not NSCs at stages later than E15, are susceptible to FoxG1-mediated temporal progression (Shen et al. 2006). In sum, the combined findings indicate that combinatorial signaling via *Smad4* and *Trim33* control cortical NSC maturation during a particular time window. Accordingly, NSCs devoid of *Smad4* and *Trim33* are not properly maturing. This function elicited by TGF $\beta$  signaling components might actually not be restricted to the forebrain. Indeed, a possible interpretation of the phenotype we observe in the midbrain is that, in the absence of TGF $\beta$

signaling, at least a part of the cells are not able to mature properly so that they lag behind in development. This would result in a temporal chimera with “younger” NSCs present in an older embryonic environment. Younger NSCs undergo more frequently symmetric divisions, exhibit a lower cell cycle exit rate, and produce less Dcx-positive neurons, in analogy to the phenotype observed in the *Smad4*-deficient midbrain. Thus, in the developing brain, TGF $\beta$  signaling might play a general role in promoting NSC maturation. In this model, area-specificity would be conferred by the local expression or activity of signaling modulators, including Trim33.

### Supplementary Material

Supplementary material can be found at: <http://www.cercor.oxfordjournals.org/>.

### Funding

This work was supported by the Swiss National Science Foundation (SNF) and by the National Center of Competence in Research “Neural Plasticity and Repair. S.F. was supported by the Neuroscience Center Zurich (ZNZ) and an SNF postdoctoral fellowship.

### Notes

We thank C. Deng, A. McMahon, and P. Soriano for providing transgenic animals and I. Miescher for valuable technical assistance. *Conflict of Interest*: None declared.

### References

- Angevine JB Jr, Sidman RL. 1961. Autoradiographic study of cell migration during histogenesis of cerebral cortex in the mouse. *Nature*. 192:766–768.
- Barnabe-Heider F, Wasylska JA, Fernandes KJ, Porsche C, Sendtner M, Kaplan DR, Miller FD. 2005. Evidence that embryonic neurons regulate the onset of cortical gliogenesis via cardiotrophin-1. *Neuron*. 48:253–265.
- Barth KA, Kishimoto Y, Rohr KB, Seydler C, Schulte-Merker S, Wilson SW. 1999. Bmp activity establishes a gradient of positional information throughout the entire neural plate. *Development*. 126:4977–4987.
- Broccoli V, Boncinelli E, Wurst W. 1999. The caudal limit of Otx2 expression positions the isthmus organizer. *Nature*. 401:164–168.
- Buchmann-Moller S, Miescher I, John N, Krishnan J, Deng CX, Sommer L. 2009. Multiple lineage-specific roles of Smad4 during neural crest development. *Dev Biol*. 330:329–338.
- Cappello S, Attardo A, Wu X, Iwasato T, Itoharu S, Wilsch-Brauninger M, Eilken HM, Rieger MA, Schroeder TT, Huttner WB et al. 2006. The Rho-GTPase cdc42 regulates neural progenitor fate at the apical surface. *Nat Neurosci*. 9:1099–1107.
- Caronia G, Wilcoxon J, Feldman P, Grove EA. 2010. Bone morphogenetic protein signaling in the developing telencephalon controls formation of the hippocampal dentate gyrus and modifies fear-related behavior. *J Neurosci*. 30:6291–6301.
- Cholfin JA, Rubenstein JL. 2007. Patterning of frontal cortex subdivisions by Fgf17. *Proc Natl Acad Sci U S A*. 104:7652–7657.
- Danielian PS, Muccino D, Rowitch DH, Michael SK, McMahon AP. 1998. Modification of gene activity in mouse embryos in utero by a tamoxifen-inducible form of Cre recombinase. *Curr Biol*. 8:1323–1326.
- Dou C, Lee J, Liu B, Liu F, Massague J, Xuan S, Lai E. 2000. BF-1 interferes with transforming growth factor beta signaling by associating with Smad partners. *Mol Cell Biol*. 20:6201–6211.
- Dupont S, Mamidi A, Cordenonsi M, Montagner M, Zacchigna L, Adorno M, Martello G, Stinchfield MJ, Soligo S, Morsut L et al. 2009. FAM/USP9x, a deubiquitinating enzyme essential for TGFbeta signaling, controls Smad4 monoubiquitination. *Cell*. 136:123–135.
- Dupont S, Zacchigna L, Cordenonsi M, Soligo S, Adorno M, Rugge M, Piccolo S. 2005. Germ-layer specification and control of cell growth by Ectodermin, a Smad4 ubiquitin ligase. *Cell*. 121:87–99.
- Falk S, Sommer L. 2009. Stage- and area-specific control of stem cells in the developing nervous system. *Curr Opin Genet Dev*. 19:454–460.
- Falk S, Wurdak H, Ittner LM, Ille F, Sumara G, Schmid MT, Draganova K, Lang KS, Paratore C, Leveen P et al. 2008. Brain area-specific effect of TGF-beta signaling on Wnt-dependent neural stem cell expansion. *Cell Stem Cell*. 2:472–483.
- Feijen A, Goumans MJ, van den Eijnden-van Raaij AJ. 1994. Expression of activin subunits, activin receptors and follistatin in postimplantation mouse embryos suggests specific developmental functions for different activins. *Development*. 120:3621–3637.
- Fukuchi-Shimogori T, Grove EA. 2001. Neocortex patterning by the secreted signaling molecule FGF8. *Science*. 294:1071–1074.
- Furuta Y, Piston DW, Hogan BL. 1997. Bone morphogenetic proteins (BMPs) as regulators of dorsal forebrain development. *Development*. 124:2203–2212.
- Gorski JA, Talley T, Qiu M, Puelles L, Rubenstein JL, Jones KR. 2002. Cortical excitatory neurons and glia, but not GABAergic neurons, are produced in the Emx1-expressing lineage. *J Neurosci*. 22:6309–6314.
- Gotz M, Huttner WB. 2005. The cell biology of neurogenesis. *Nat Rev Mol Cell Biol*. 6:777–788.
- Grove EA, Tole S, Limon J, Yip L, Ragsdale CW. 1998. The hem of the embryonic cerebral cortex is defined by the expression of multiple Wnt genes and is compromised in Gli3-deficient mice. *Development*. 125:2315–2325.
- Hanashima C, Fernandes M, Hebert JM, Fishell G. 2007. The role of Foxg1 and dorsal midline signaling in the generation of Cajal-Retzius subtypes. *J Neurosci*. 27:11103–11111.
- Hanashima C, Li SC, Shen L, Lai E, Fishell G. 2004. Foxg1 suppresses early cortical cell fate. *Science*. 303:56–59.
- Haubensack W, Attardo A, Denk W, Huttner WB. 2004. Neurons arise in the basal neuroepithelium of the early mammalian telencephalon: a major site of neurogenesis. *Proc Natl Acad Sci USA*. 101:3196–3201.
- He W, Dorn DC, Erdjument-Bromage H, Tempst P, Moore MA, Massague J. 2006. Hematopoiesis controlled by distinct TIF1gamma and Smad4 branches of the TGFbeta pathway. *Cell*. 125:929–941.
- Hebert JM, Hayhurst M, Marks ME, Kulesa H, Hogan BL, McConnell SK. 2003. BMP ligands act redundantly to pattern the dorsal telencephalic midline. *Genesis*. 35:214–219.
- Hebert JM, Mishina Y, McConnell SK. 2002. BMP signaling is required locally to pattern the dorsal telencephalic midline. *Neuron*. 35:1029–1041.
- Hirabayashi Y, Suzuki N, Tsuboi M, Endo TA, Toyoda T, Shinga J, Koseki H, Vidal M, Gotoh Y. 2009. Polycomb limits the neurogenic competence of neural precursor cells to promote astrogenic fate transition. *Neuron*. 63:600–613.
- Kim J, Kaartinen V. 2008. Generation of mice with a conditional allele for Trim33. *Genesis*. 46:329–333.
- Ko SO, Chung IH, Xu X, Oka S, Zhao H, Cho ES, Deng C, Chai Y. 2007. Smad4 is required to regulate the fate of cranial neural crest cells. *Dev Biol*. 312:435–447.
- Kriegstein A, Alvarez-Buylla A. 2009. The glial nature of embryonic and adult neural stem cells. *Annu Rev Neurosci*. 32:149–184.
- Massague J. 2008. TGFbeta in Cancer. *Cell*. 134:215–230.
- Miller FD, Gauthier AS. 2007. Timing is everything: making neurons versus glia in the developing cortex. *Neuron*. 54:357–369.
- Miyata T, Kawaguchi A, Saito K, Kawano M, Muto T, Ogawa M. 2004. Asymmetric production of surface-dividing and non-surface-dividing cortical progenitor cells. *Development*. 131:3133–3145.
- Morsut L, Yan KP, Enzo E, Aragona M, Soligo SM, Wendling O, Mark M, Khetchoumian K, Bressan G, Chambon P et al. 2010. Negative

- control of Smad activity by ectodermin/Tif1gamma patterns the mammalian embryo. *Development*. 137:2571–2578.
- Namihira M, Kohyama J, Semi K, Sanosaka T, Deneen B, Taga T, Nakashima K. 2009. Committed neuronal precursors confer astrocytic potential on residual neural precursor cells. *Dev Cell*. 16:245–255.
- Noctor SC, Martinez-Cerdeno V, Ivic L, Kriegstein AR. 2004. Cortical neurons arise in symmetric and asymmetric division zones and migrate through specific phases. *Nat Neurosci*. 7:136–144.
- Okano H, Temple S. 2009. Cell types to order: temporal specification of CNS stem cells. *Curr Opin Neurobiol*. 19:112–119.
- O'Leary DD, Chou SJ, Sahara S. 2007. Area patterning of the mammalian cortex. *Neuron*. 56:252–269.
- Rakic P. 2009. Evolution of the neocortex: a perspective from developmental biology. *Nat Rev Neurosci*. 10:724–735.
- Rakic P. 1974. Neurons in rhesus monkey visual cortex: systematic relation between time of origin and eventual disposition. *Science*. 183:425–427.
- Rakic P. 1995. A small step for the cell, a giant leap for mankind: a hypothesis of neocortical expansion during evolution. *Trends Neurosci*. 18:383–388.
- Rakic P. 1988. Specification of cerebral cortical areas. *Science*. 241:170–176.
- Roussa E, Wiehle M, Dunker N, Becker-Katins S, Oehlke O, Kriegstein K. 2006. Transforming growth factor beta is required for differentiation of mouse mesencephalic progenitors into dopaminergic neurons in vitro and in vivo: ectopic induction in dorsal mesencephalon. *Stem Cells*. 24:2120–2129.
- Rowitch DH, McMahon AP. 1995. Pax-2 expression in the murine neural plate precedes and encompasses the expression domains of Wnt-1 and En-1. *Mech Dev*. 52:3–8.
- Seoane J, Le HV, Shen L, Anderson SA, Massague J. 2004. Integration of Smad and forkhead pathways in the control of neuroepithelial and glioblastoma cell proliferation. *Cell*. 117:211–223.
- Seuntjens E, Nityanandam A, Miquelajauregui A, Debruyjn J, Stryjewska A, Goebbels S, Nave KA, Huylebroeck D, Tarabykin V. 2009. Sip1 regulates sequential fate decisions by feedback signaling from post-mitotic neurons to progenitors. *Nat Neurosci*. 12:1373–1380.
- Shen Q, Wang Y, Dimos JT, Fasano CA, Phoenix TN, Lemischka IR, Ivanova NB, Stifani S, Morrisey EE, Temple S. 2006. The timing of cortical neurogenesis is encoded within lineages of individual progenitor cells. *Nat Neurosci*. 9:743–751.
- Shimamura K, Rubenstein JL. 1997. Inductive interactions direct early regionalization of the mouse forebrain. *Development*. 124:2709–2718.
- Shimogori T, Banuchi V, Ng HY, Strauss JB, Grove EA. 2004. Embryonic signaling centers expressing BMP, WNT and FGF proteins interact to pattern the cerebral cortex. *Development*. 131:5639–5647.
- Soriano P. 1999. Generalized lacZ expression with the ROSA26 Cre reporter strain. *Nat Genet*. 21:70–71.
- Truett GE, Heeger P, Mynatt RL, Truett AA, Walker JA, Warman ML. 2000. Preparation of PCR-quality mouse genomic DNA with hot sodium hydroxide and tris (HotSHOT). *Biotechniques*. 29: 52, 54.
- Xi Q, Wang Z, Zaromytidou AI, Zhang XH, Chow-Tsang LF, Liu JX, Kim H, Barlas A, Manova-Todorova K, Kaartinen V et al. 2011. A poised chromatin platform for TGF-beta access to master regulators. *Cell*. 147:1511–1524.
- Yang X, Li C, Herrera PL, Deng CX. 2002. Generation of Smad4/Dpc4 conditional knockout mice. *Genesis*. 32:80–81.
- Yoshida M, Assimacopoulos S, Jones KR, Grove EA. 2006. Massive loss of Cajal-Retzius cells does not disrupt neocortical layer order. *Development*. 133:537–545.